

Original Article

**Effects of orientation and density of thermoplastic polyurethane honeycomb print
on impact response in footwear and absorption applications**

Satta Srewaradachpibal^{1,4,5}, Surapong Chatpun², Muhammad Nouman³, and Wiriya
Thongruang^{1,4*}

¹Department of Mechanical Engineering, Faculty of Engineering, Prince of Songkla
University, Hat Yai, Songkhla 90112, Thailand

²Department of Biomedical Sciences and Biomedical Engineering, Faculty of Medicine,
Prince of Songkla University, Hat Yai, Songkhla 90110, Thailand

³Sirindhorn School of Prosthetics and Orthotics, Faculty of Medicine, Siriraj Hospital,
Mahidol University, Bangkok 10700, Thailand

⁴Smart Industry Research Center, Department of Industrial and Manufacturing
Engineering Faculty of Engineering, Prince of Songkla University, Hatyai Campus,
Songkhla 90110, Thailand

⁵Center of Excellence in Metal and Materials Engineering, Prince of Songkla
University, Hatyai Campus, Songkhla 90110, Thailand

***Corresponding author, Email address: satta.s@psu.ac.th**

Abstract

This study examined how 3D printing might increase impact force reduction in footwear application. The study used 3D honeycomb constructions constructed of thermoplastic polyurethane to show how print orientation and density affect footwear's sensitivity to impact energy. Thorough characterization and standardized testing are used to analyze 3D- printed honeycomb lattice mechanical properties. This showed that construction orientation and density affect stiffness and elasticity. The fundamental

investigation of this study revolved around the crucial relationship between construction orientations and density, which affect impact force dissipation. The transverse structure exhibited the highest impact reduction efficiency of 0.75 in our analysis, whereas the remaining structures only managed 0.65. Conversely, the impact reduction was significantly more influenced by the appropriate structural density than by the orientation angle. Impact mitigation and absorption applications can be enhanced through the use of 3D honeycomb TPU printing, which enables manufacturers to create comfortable protection.

Keywords: 3D printing TPU; Impact force; Footwear; Hip-protector; Honeycomb orientation angle

1. Introduction

The impact forces experienced during physical activities can significantly impact the health and comfort of individuals wearing shoes (Mercer & Horsch, 2015; O’Leary et al., 2008; Price et al., 2014; Silva et al., 2009). Insufficient absorption and mitigation of these forces by footwear can lead to discomfort, fatigue, and even prolong injuries. To address this concern, footwear manufacturers have been incorporating specialized functions and technologies into their products to enhance impact protection (Dib et al., 2005; O’Leary et al., 2008; Silva et al., 2009).

One crucial component responsible for cushioning in footwear is the midsole, which plays a vital role in reducing the impact forces transmitted to the feet and lower extremities. Traditional materials used for midsole production include Ethylene-vinyl acetate (EVA), polyurethane (PU) foam, and other elastic materials (Brückner et al., 2010; Heidenfelder et al., 2009; Lipka et al., 2014; Silva et al., 2009; Speed et al., 2018;

Verdejo & Mills, 2004). These materials must possess essential features such as effective impact reduction and lightweight properties.

While traditional manufacturing methods limit the creation of complex internal structures in shoe soles, three-dimensional (3D) printing technology has emerged as a promising solution. 3D printing has revolutionized the manufacturing industry, enabling the production of diverse products with varying properties such as hardness, compressive strength, and energy absorption (Bates et al., 2016). The structure of the printed object also plays a crucial role in impact force reduction. One material that has been investigated for 3D printing is thermoplastic polyurethane (TPU), known for its flexibility and resilience.

One particular intriguing structure is the honeycomb pattern, which mimics natural designs found in nature. The mechanical properties of honeycomb structures vary depending on the orientation of the printing angles. Previous studies have examined the impact force reduction of 3D-printed TPU honeycomb structures (Bates et al., 2016, 2019). However, the impact strength of these structures with different orientations has not been thoroughly investigated. Prior research has exclusively examined compressive stress structure in two directions: transverse and ribbon. Ribbon structures have been observed to be more robust and absorb more energy than transverse structures. (Bates et al., 2019; Habib, 2020) Moreover, there is an absence of research examining the effect that structural rotation has on impact force reduction. The mechanical properties of the structure are influenced by its density. An investigation has been conducted to determine the material's resistance to impact. However, the parameters of evaluation differ in accordance with the particular application (Bates et al., 2019; Habib, 2020; Rahman et al., 2022; Rahman & Koohbor, 2020; Ramirez & Gupta, 2019). Therefore, previous

research has lacked information on the impact parameter of honeycomb structures with different orientation angles and densities.

This study advances footwear industry knowledge of 3D printing and TPU designs. Thus, this study focused on understanding the honeycomb orientations and structure densities that minimize impact forces to enable the development of novel, high-performance footwear that emphasizes wearer health and comfort. It can also be applied to other industries that involve impact protection, such as hip protectors or lightweight helmets.

2. Materials and Methods

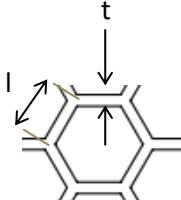
2.1. TPU property and 3D printer

TPU (PolyFlex™ TPU95) was purchased from Palawat Automation Co., Ltd. (Nakhon Pathom, Thailand). TPU has density 1.20 g/cm^3 and melt index 3-6 g with 210 °C, 1.2 kg. The mechanical property of TPU is shown in Table 1. The three-dimensional custom printer was used in the experiment with the base size width \times length \times height equal to $200 \times 200 \times 200$ millimeters, and nozzle size of 0.5 millimeters, with the printing resolution range 0.05-0.4 millimeters. The Ultimaker Cura 4.2.1 was used to generate G-code for printing. Similar conditions were followed to 3D print TPU honeycomb as shown in Table 2.

2.2 3D printing design

Honeycomb pattern was designed with SolidWorks 2021 software from Applied Public Company Limited. The wall thickness of 0.75 mm was kept the same with different density $0.24\text{-}0.48 \text{ g/cm}^3$ by variable wall-length values between 1.80 and 3.54 mm. The honeycombs were three orientations of structure at Ribbon (0°C), Tran-Rib (15°C) and

Transverse (30°C) as shown in Table 3. TPU honeycomb was printed in size 60 x 60 x10 mm. The determination of the relative density (ρ_{RD}) of a honeycomb structure can be achieved by employing the cell wall length l and thickness t . The relationship between the thickness and length of cells and their relative density is depicted in Equation 1. Furthermore, the ratio denoted as " t/l " is a component of a hexagonal unit cell. The equation provided represents the relative density of a hexagonal array in which the length varies while the wall thickness remains constant (Bates et al., 2019).



$$\rho_{RD} = \left(\frac{2}{\sqrt{3}}\right)\left(\frac{t}{l}\right) \quad \text{Eq.1}$$

2.3 Mechanical properties (compression tests)

The specimens' compressive properties were tested using an Instron 8872 from Instron (Thailand) with loadcell 25kN equipment. The square specimen has a length of 50 mm and a thickness of 10 mm. The testing machine compressed the specimens at 70% strain with a constant cross-head speed of 10 mm/min. This yielded a constant strain rate of 0.01 s^{-1} . The stress and strain relations were obtained from the testing results.

2.4 Impact properties (drop test)

Shock absorption was evaluated in accordance with ASTM- F1614 using a custom-built drop-testing machine, as shown in Figure 1. The thickness of the test specimens of molded samples was maintained at 10 mm. On each specimen, an 8.5 kg striker with a 45 mm diameter was dropped from 36 to 84 mm (depending on the impact energy of 3–7 joules) [20–22]. The impact force was measured with a Kyowa Dengyo

(Thailand) accelerometer model: ASH-A-100, and the specimen collapse distance was measured with a Kyowa Dengyo (Thailand) laser distance sensor model: AXIS-HP-200-1. The data was processed, recorded, and analyzed. The acceleration data was converted into impact force values by multiplying it with the mass (8.5kg). These impact acceleration values were then used to calculate the impact cushioning efficiency (ICE) using Equation 2. The impact acceleration at *Solid TPU* g_{max} was assessed on 100% solid TPU, which denotes the complete printing of the TPU material, and *Honeycomb* g_{max} honeycomb g_{max} , which represents the impact acceleration value examined across a range of honeycomb structure types.

$$\text{Impact cushioning efficiency (ICE)} = \frac{\text{Solid TPU } g_{max} - \text{Honeycomb } g_{max}}{\text{Solid TPU } g_{max}} \quad \text{Eq.2}$$

3. Results and Discussion

3.1. Specimen quality

The Ultimaker Cura 4.3.0 software generated a G-code file to print the specimens. A controlled and consistent printing process was achieved at 30 mm/s. The specimens' infill structure was exact and detailed because of the 0.1 mm line pattern infill layer thickness. The material was printed at 228 °C to ensure effective printing. TPU flow and adhesion during printing are optimized at this temperature. To improve print adherence, the build plate was heated to 50 °C (Lopes et al., 2018). This study used three samples per design and found the same tendency (Basurto-Vázquez et al., 2021). Every sample is high-quality and produces reliable test results.

Figure 2a shows vertically layered specimens with a 0.31 ρRD. Interior infill density is the amount of material used to fill the printed object. In this situation, 100%

infill density maximizes specimen strength and density by creating a solid framework. The sample's precise and consistent printing laid the groundwork for mechanical property research. Some of the specimens in Figure 2b are excellent. Table 4 lists these specimens' weight, size, and density. The specimens have the same 10 mm thickness, 60 mm width, and 60 mm length. Honeycomb structures with comparable relative density had similar physical properties in various orientations. A detailed study of the workpiece's size, weight, and dimensions shows an exceedingly small variance. These items with a higher relative density are heavier. According to prior investigations, honeycomb samples weighed 15–25 g and had a density of 0.4–0.70 g/cm³ (Basurto-Vázquez et al., 2021; Bates et al., 2016, 2019).

3.2 Compression behavior of TPU honeycomb

Under the loading conditions depicted in Figure 3, the compressive force of 3D printed TPU structures with varying densities were evaluated. Each structure demonstrates three unique deformation stages: linear elasticity, plateau, and densification (Bates et al., 2016, 2019; Li et al., 2019). During initial compressive strains, the behavior is linear due to simple elastic of the structure's cell walls. The cell walls buckle as deformation continues, culminating in the characteristic plateau phase. Densification occurs when the opposing cell walls eventually come into contact. The rigidity of the structure experiences a substantial increase during this densification phase, nearly reaching the stiffness of the initial solid material (Tomin & Kmetty, 2022).

Figure 3a initiates the comparison of 3D honeycomb structures at different densities by focusing on transversely oriented honeycomb structures across three density levels. The results of this study agree with previous research that has examined the compressive properties of dense structures (Bates et al., 2019; Tomin & Kmetty, 2022).

Dense structures exhibit superior compressive characteristics. Notably, the high-density TPU 3D printing (RD 0.48) is of great structural strength. Furthermore, these structures exhibit exceptionally high energy adsorption capacities, as evidenced by the area under the stress-strain relationship curve. This value increases as the density of the structure increases. Due to their dimensions, structures with a high relative density have a reduced plateau stress range (Basurto-Vázquez et al., 2021; Bates et al., 2019; Rahman & Koohbor, 2020). As cellular dimensions decrease, there is a corresponding contraction of the intercellular space. So the value of the distance at which densification occurs decreases in correlation with the relative density value. Figure 3b demonstrated that altering the angle of the 3D structure affects its compressive properties. The results indicated the compressive capacity of Ribbon and Tran-Rib structures is nearly identical, with ribbon angles being slightly more acute. On the other hand, the transverse structure with a trans angle exhibited the lowest compressive strength. Also, the transverse structure has a wider stress plateau range than other structures (Bates et al., 2016, 2019; Habib, 2020). This means that the trans-angle structure can collapse more quickly than other angles with the same density. The observed differences in compressive properties due to density variations and structural angles provide valuable insights for understanding the mechanical behavior of 3D-printed honeycomb structures.

Compressive characteristics varied with honeycomb structures of varying densities and angles. Compressive stress increased with density, while structural angles affected compressive capacity. These findings help footwear product development by explaining cushioning-related mechanical features.

3.3 Dynamic behavior of TPU honeycomb (Force, Time and Displacement)

Impact test results conducted in accordance with ASTM-F1614 standards provide essential data about a material's or structure's response to impact (Srewaradachpisal et al., 2020). These results usually include important data such as impact value, which quantifies the force exerted during the impact, timing, and collapse distance, which measures how far the sample deforms or collapses under the impact force. ASTM- F1614 ensures consistency and reliability when evaluating materials and products. A small impact force indicates effective impact absorption, while the collapse distance indicates how much the material or product must bend to absorb impact energy.

Figure 4a. illustrates the impact attenuation test results of the workpieces having different relative densities. The Solid TPU 100% demonstrates the highest impact force and the least amount of cushioning. Obviously, although the workpieces possess the same honey comb structure, density of the sample significantly affected the impact attenuation. Here, the displacement decreased with the increased density. The samples (RD-0.24 and RD-0.48) still had high impact force, indicating low shock absorption. The medium relative density (RD-0.36) showed the lowest impact force, indicating high absorption of the impact energy. The observed variations in impact behavior among the samples can be linked to their distinct mechanical properties, as illustrated in Figure 3a in comparison to Figure 4b. Sample RD-0.36 collapsed within a plateau region, similar to RD-0.48, which also experienced plateau collapse but at a higher force due to its strong structure. RD-0.24 collapsed within a densification region, surpassing the plateau stress region. Comparatively, research on the impact force of honeycomb structures yields consistent results indicating that the impact reduction is influenced differently by the density of honeycomb structures (Bates et al., 2019). This variation can be attributed to the distinct mechanical properties of the honeycomb structures (Srewaradachpisal et al., 2020). In

order to ascertain the optimal density of structures for implementation in practical contexts, experimentation is therefore necessary (Rahman et al., 2022). The selection of an optimal density gradient may be necessary in applications that demand a wide range of impact energies, dependent upon the specific design criteria and application at hand (Bates et al., 2019; Rahman et al., 2022; Rahman & Koohbor, 2020).

Figure 4c. illustrates the impact attenuation test results of the workpieces having different angle orientation of structures. It was found that the angle orientation had a slight effect on the impact attenuation. The study revealed that structures oriented at transverse angles demonstrated the most effective reduction in impact forces. Additionally, within this density range, Ribbon and Rib-Tran angles exhibited comparable abilities to decrease forces. This observation aligns with the compressive properties depicted in Figure 3b, where Ribbon and Rib-Tran structures displayed similar mechanical characteristics. Previous research was solely concerned with comparing the mechanical properties of ribbon and transverse honeycomb structures (Bates et al., 2016, 2019). This research has thus revealed distinctions in the impact characteristics of structures oriented at various angles that were previously unknown. Among them, the sample with transvers angle undergo the largest displacement in Figure 4d. As compared to the relative density of samples, it is clear that the angle orientation showed less effect on the impact properties.

3.4 Dynamic behavior in varies impact energy

Spline curve graphs evaluated structures with 3–7 joules of impact energy. Throughout the testing, these graphs showed the relationship between impact force, collapse distance (displacement), and structural relative density. These results highlight the importance of optimizing structure density to absorb impact forces within the prescribed energy range. Figure 5 shows the importance of density customization in

designing and developing structures that can absorb impact forces in the prescribed test energy range.

Upon examining the honeycomb structures under various impact energy levels, as shown in Figures 5a, 5c, and 5e for transverse, trans-rib, and ribbon orientations respectively, it was evident that higher impact energies led to increased impact forces (Bates et al., 2019; Ramirez & Gupta, 2019; Srewaradachpisal et al., 2020). The study identified optimal density values that effectively minimized these impact forces: 0.31, 0.36, and 0.41 for transverse structures. For trans-rib structures, the most efficient density values varied with impact energy levels, being 0.31-0.36, 0.36, and 0.41, respectively. Similarly, for ribbon structures, the most effective density value was consistently found to be 0.36 across impact energies of 3, 5, and 7 joules. Different structural orientations resulted in varying densities that are effective in reducing impact forces. Furthermore, different impact energies also lead to different optimal densities for efficient impact reduction.

When considering the collapse distances (displacement) of the structures under impact, as illustrated in Figures 5b, 5d, and 5f, it was observed that at the same impact energy level, structures with lower density experienced greater collapse distances compared to those with higher density (Ramirez & Gupta, 2019). Besides, it was evident that higher impact energies led to greater collapse distances (displacement). Upon examining all figures, it becomes evident that the reduction in impact force is directly related to the collapse distance. Structures that collapse more can effectively mitigate impact forces. However, if the structure's density is excessively low, it might collapse significantly and fail to absorb the impact force effectively, unable to accommodate the energy. In such cases, the structure collapses into the plateau stress region and transitions

into the densification phase, akin to the behavior observed in Figure 4 a. These findings demonstrate the complicated relationship between impact energy, structural density, and collapse distance, contributing to the design and optimization of honeycomb structures to absorb impact forces at varied energy levels.

The Figure 6 displays the results from impact tests conducted within the 3-7 joules range of impact energy. These results are compared to the relative density of honeycomb structures at different angles. As depicted in Figure 6a, it is noticeable that, at an impact energy level of 3 joules, the transverse, ribbon, and trans-rib honeycomb structures demonstrated superior damping performance at relative densities within the range of 0.31-0.36 similarly. Notably, among these structures, the transverse design clearly outperforms others in reducing loads.

In Figure 6b, the impact cushioning efficiency comparing solid TPU was demonstrated. The analysis revealed that different structural designs led to varying impact absorption efficiencies. Transverse-oriented structures reduced impact better than other structures, with an efficiency of 0.75 compared to 0.65. Less dense materials absorb shock better than denser ones, with 0.48–0.58 and 0.42–0.48 efficiency, respectively. At this impact energy, lower densities absorb impact better than higher densities.

Figure 6c shows that impact forces at 5 joules of impact energy followed the same patterns as at 3 joules. Transverse-oriented structures reduced impact effectively. The optimal density for impact reductions remained 0.36. In Figure 6d, transverse structures at 0.36 density had a greater impact reduction efficiency of 0.75 than other structures at 0.6. It becomes apparent that higher densities in this energy range are more efficient in impact reduction compared to lower density ranges.

In Figure 6e, similar to previous observations, the transverse-oriented structures continue to demonstrate the best impact reduction capabilities within the density range of 0.41. Figure 6f illustrates the diminishing impact reduction efficiency. In this scenario, transverse structures maintain their superior impact reduction efficiency, scoring 0.62, while other designs only achieve an efficiency level of 0.55 at this specific impact energy level. Additionally, it becomes evident that higher density ranges exhibit better impact reduction capabilities compared to lower density ranges.

4. Conclusions

In this research, it was discovered that the honeycomb structure with a transverse orientation demonstrated superior impact reduction capabilities across all energy impact scenarios. Regarding the trans-rib and ribbon orientations, they exhibited similar impact attenuation. Notably, this configuration boasted the lowest density, making it an excellent choice for manufacturing lightweight impact-resistant components. Additionally, it incurred lower production expenses compared to high-density counterparts. The experiments indicated that low-density structures proved more efficient at mitigating impacts under low impact energy conditions. Conversely, high-density structures proved more effective in absorbing impacts during high impact energy scenarios. As a result, structure density should be prioritized over structure orientation when choosing a honeycomb for shock absorption.

Acknowledgments

This research was supported by National Science, Research and Innovation Fund (NSRF) and Prince of Songkla University (Ref. No. MED6701005a). The authors would

like to thank the Department of Mechanical Engineering, Faculty of Engineering, the Department of Biomedical Sciences and Biomedical Engineering, Faculty of Medicine, Prince of Songkla University, Thailand for the provision of the experimental facilities in the research.

References

- Basurto-Vázquez, O., Sánchez-Rodríguez, E. P., McShane, G. J., & Medina, D. I. (2021). Load distribution on pet- g 3d prints of honeycomb cellular structures under compression load. *Polymers*, *13*(12), 1–13. <https://doi.org/10.3390/polym13121983>
- Bates, S. R. G., Farrow, I. R., & Trask, R. S. (2016). 3D printed polyurethane honeycombs for repeated tailored energy absorption. *Materials and Design*, *112*, 172– 183. <https://doi.org/10.1016/j.matdes.2016.08.062>
- Bates, S. R. G., Farrow, I. R., & Trask, R. S. (2019). Compressive behaviour of 3D printed thermoplastic polyurethane honeycombs with graded densities. *Materials and Design*, *162*, 130–142. <https://doi.org/10.1016/j.matdes.2018.11.019>
- Brückner, K., Odenwald, S., Schwanitz, S., Heidenfelder, J., & Milani, T. (2010). Polyurethane- foam midsoles in running shoes - Impact energy and damping. *Procedia Engineering*, *2*(2) , 2789– 2793. <https://doi.org/10.1016/j.proeng.2010.04.067>
- Dib, M. Y., Smith, J., Bernhardt, K. A., Kaufman, K. R., & Miles, K. A. (2005). Effect of environmental temperature on shock absorption properties of running shoes. *Clinical Journal of Sport Medicine*, *15*(3) , 172– 176. <https://doi.org/10.1097/01.jsm.0000165348.32767.32>

- Habib, F. N. (2020). *Development of High Performing 3D Printed Polymeric Cellular Structures for Wearable Impact Protection* (Issue July). School of Engineering, Faculty of Science, Engineering and Technology Swinburne University of Technology Melbourne, Australia.
- Heidenfelder, J., Sterzing, T., & Milani, T. L. (2009). Biomechanical wear testing of running shoes. *Footwear Science*, *1*(September 2016) , 16– 17. <https://doi.org/10.1080/19424280902977046>
- Li, D., Liao, W., Dai, N., & Xie, Y. M. (2019). *Absorption of Sheet-Based and Strut-Based Gyroid*.
- Lippa, N., Hall, E., Piland, S., Gould, T., & Rawlins, J. (2014). Mechanical ageing protocol selection affects macroscopic performance and molecular level properties of ethylene vinyl acetate (EVA) running shoe midsole foam. *Procedia Engineering*, *72*(Mills 2007), 285–291. <https://doi.org/10.1016/j.proeng.2014.06.082>
- Lopes, L. R., Silva, A. F., & Carneiro, O. S. (2018). Multi-material 3D printing: The relevance of materials affinity on the boundary interface performance. *Additive Manufacturing*, *23*(March), 45–52. <https://doi.org/10.1016/j.addma.2018.06.027>
- Mercer, J. A., & Horsch, S. (2015). Heel-toe running: A new look at the influence of foot strike pattern on impact force. *Journal of Exercise Science and Fitness*, *13*(1), 29–34. <https://doi.org/10.1016/j.jesf.2014.12.001>
- O’Leary, K., Vorpahl, K. A., & Heiderscheidt, B. (2008). Effect of cushioned insoles on impact forces during running. *Journal of the American Podiatric Medical Association*, *98*(1), 36–41. <https://doi.org/10.7547/0980036>
- Price, C., Cooper, G., Graham-Smith, P., & Jones, R. (2014). A mechanical protocol to

- replicate impact in walking footwear. *Gait and Posture*, 40(1) , 26– 31.
<https://doi.org/10.1016/j.gaitpost.2014.01.014>
- Rahman, O., & Koohbor, B. (2020). Optimization of energy absorption performance of polymer honeycombs by density gradation. *Composites Part C: Open Access*, 3(August), 100052. <https://doi.org/10.1016/j.jcomc.2020.100052>
- Rahman, O., Uddin, K. Z., Muthulingam, J., Youssef, G., Shen, C., & Koohbor, B. (2022). Density-Graded Cellular Solids: Mechanics, Fabrication, and Applications. *Advanced Engineering Materials*, 24(1) , 1– 20.
<https://doi.org/10.1002/adem.202100646>
- Ramirez, B. J., & Gupta, V. (2019). Energy Absorption and Low Velocity Impact Response of Open-Cell Polyurea Foams. *Journal of Dynamic Behavior of Materials*, 5(2), 132–142. <https://doi.org/10.1007/s40870-019-00192-0>
- Silva, R. M., Rodrigues, J. L., Pinto, V. V., Ferreira, M. J., Russo, R., & Pereira, C. M. (2009). Evaluation of shock absorption properties of rubber materials regarding footwear applications. *Polymer Testing*, 28(6) , 642– 647.
<https://doi.org/10.1016/j.polymertesting.2009.05.007>
- Speed, G., Harris, K., & Keegel, T. (2018). The effect of cushioning materials on musculoskeletal discomfort and fatigue during prolonged standing at work: A systematic review. *Applied Ergonomics*, 70(February) , 300– 314.
<https://doi.org/10.1016/j.apergo.2018.02.021>
- Srewaradachpaisal, S., Dechwayukul, C., Chatpun, S., Spontak, R. J., & Thongruang, W. (2020). Optimization of the rubber formulation for footwear applications from the response surface method. *Polymers*, 12(9) , 7– 11.

<https://doi.org/10.3390/POLYM12092032>

Tomin, M., & Kmetty, Á. (2022). Polymer foams as advanced energy absorbing materials for sports applications—A review. *Journal of Applied Polymer Science*, 139(9), 1–23. <https://doi.org/10.1002/app.51714>

Verdejo, R., & Mills, N. J. (2004). Heel-shoe interactions and the durability of EVA foam running- shoe midsoles. *Journal of Biomechanics*, 37(9) , 1379– 1386. <https://doi.org/10.1016/j.jbiomech.2003.12.022>

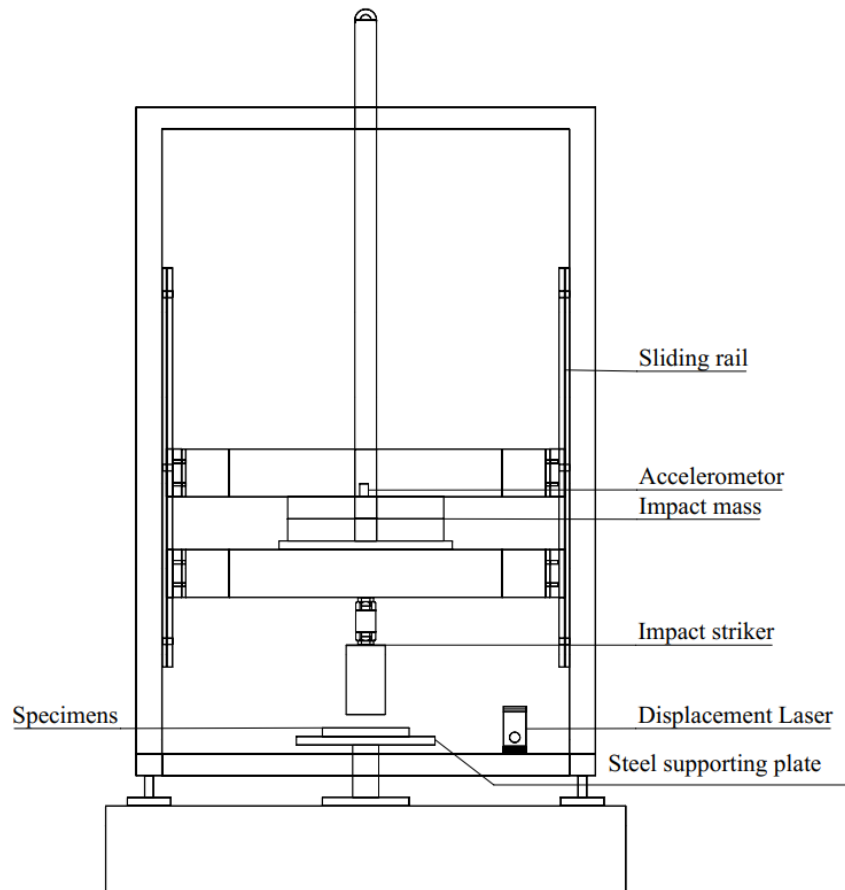


Figure 1 The custom-built drop-testing machine used to measure impact energy

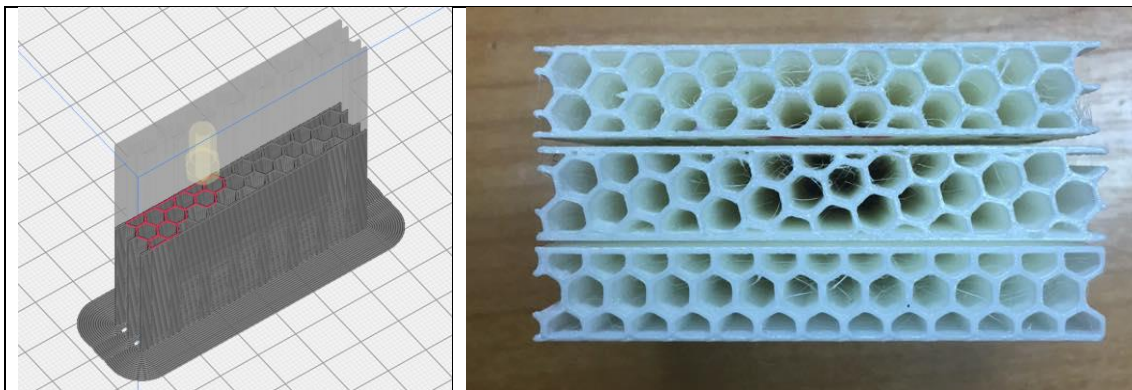


Figure 2 a) The printing path of the honeycomb structure, b) the TPU-printed honeycomb structure's quality (ρ_{RD} 0.31) in three different orientations (Top Ribbon, Middle Tran-Rib, and Bottom Transverse).

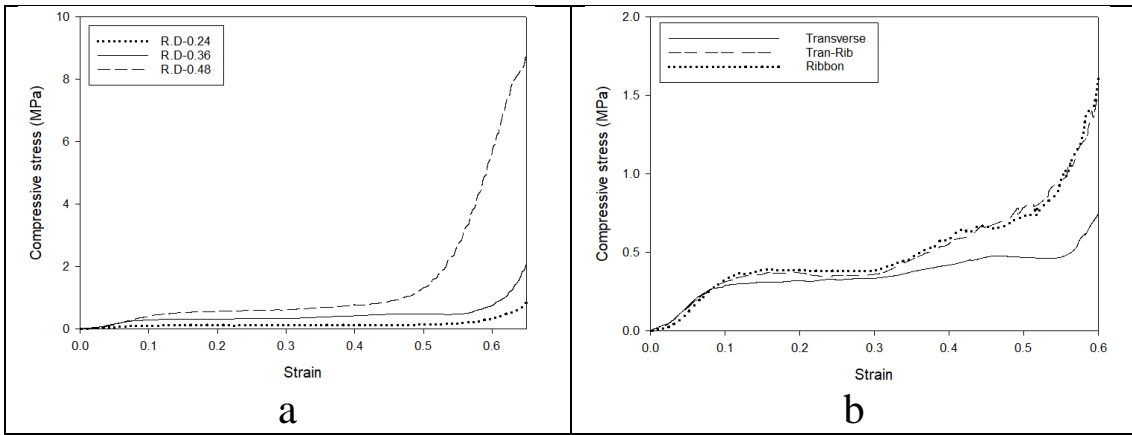


Figure 3 Three honeycombs structure printed from TPU a) Transverse angle in varies ρ_{RD} ; b) $\rho_{RD} = 0.36$ in varies angle

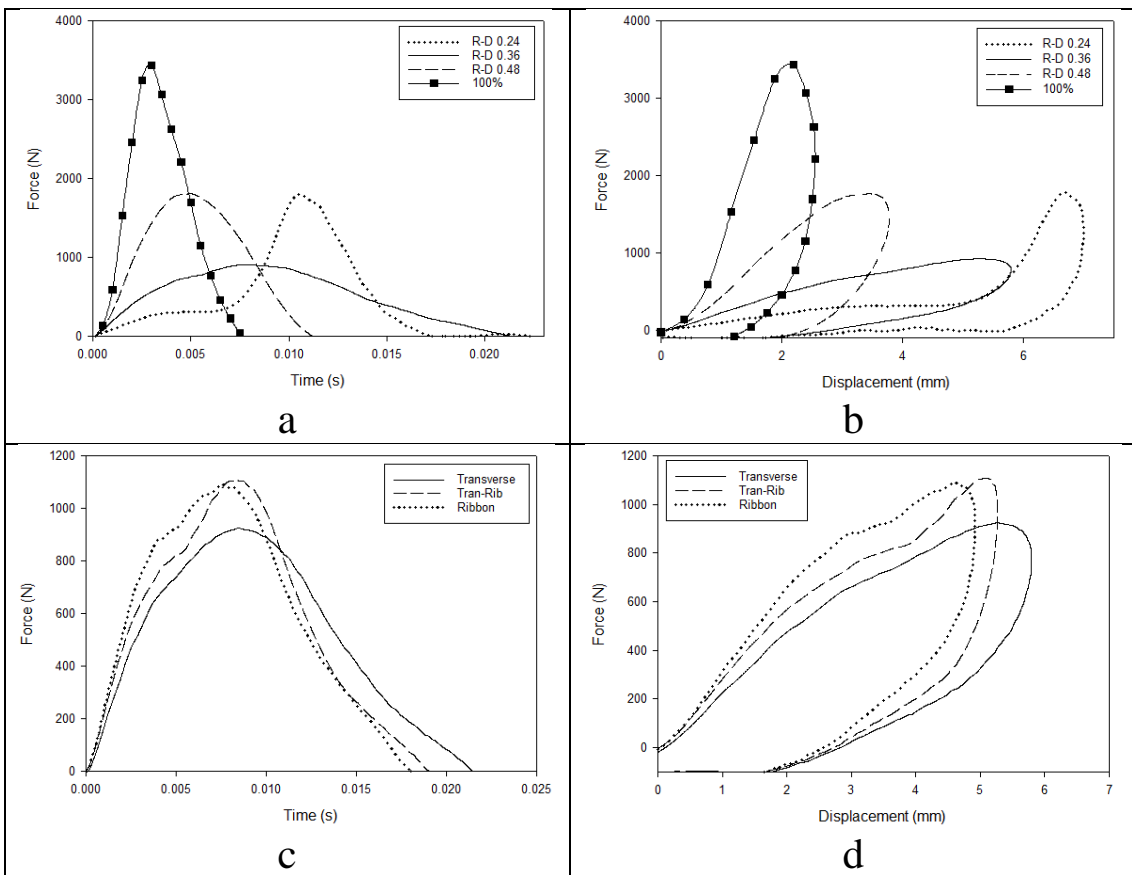


Figure 4 Drop test result from TPU honeycomb in Transverse angle by varies ρ_{RD} a) force vs time b) force vs displacement, in $\rho_{RD} = 0.36$ by varies angle c) force vs time d) force vs displacement

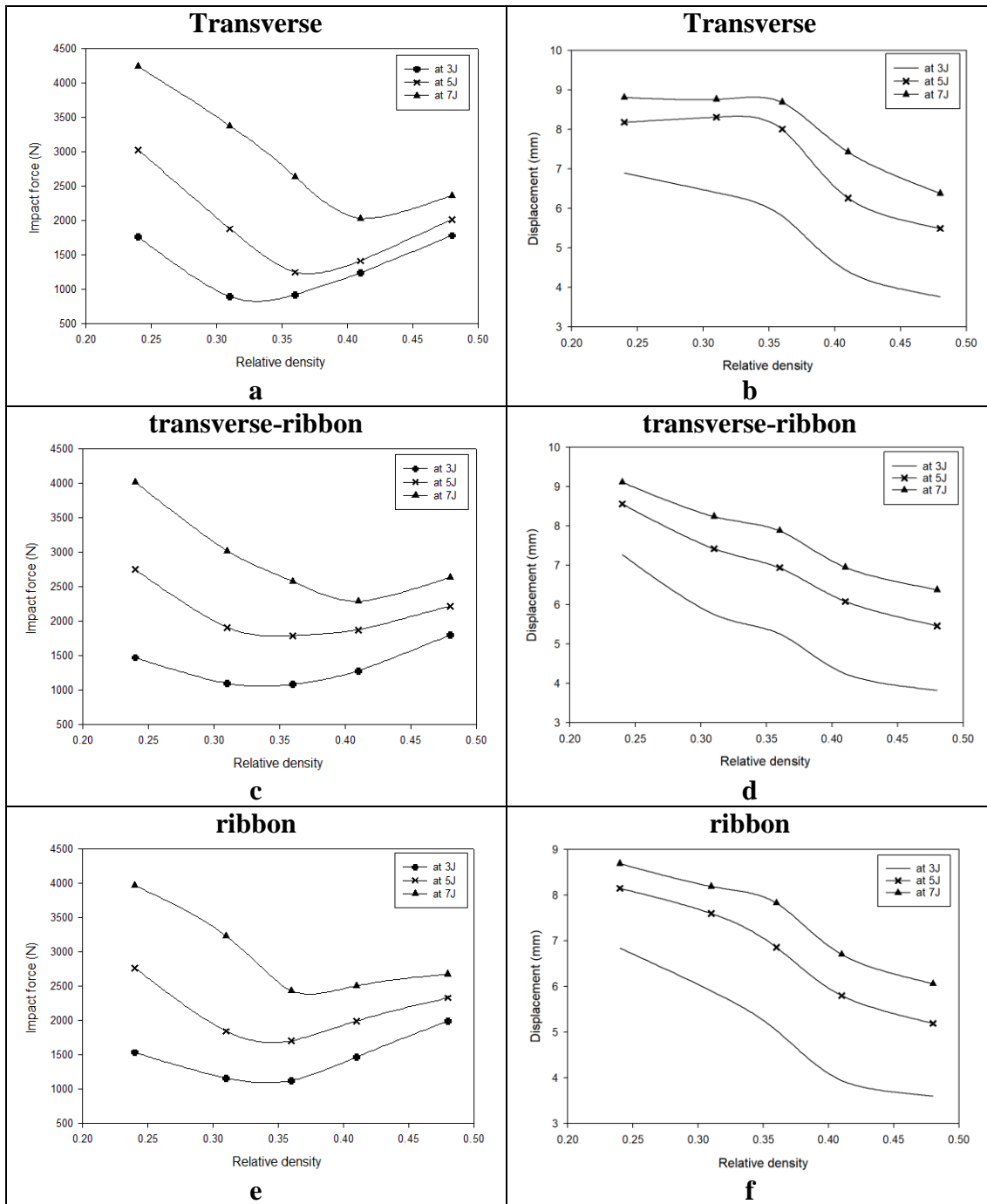


Figure 5 The impact of honeycomb structure orientation on varies energy. a) Depicts the transverse impact force versus relative density (ρ_{RD}). b) Represents transverse displacement in relation to ρ_{RD} . c) Displays trans-rib impact force versus ρ_{RD} . d) Shows trans-rib displacement concerning ρ_{RD} . e) Illustrates ribbon impact force versus ρ_{RD} . and f) Exhibits ribbon displacement versus ρ_{RD} .

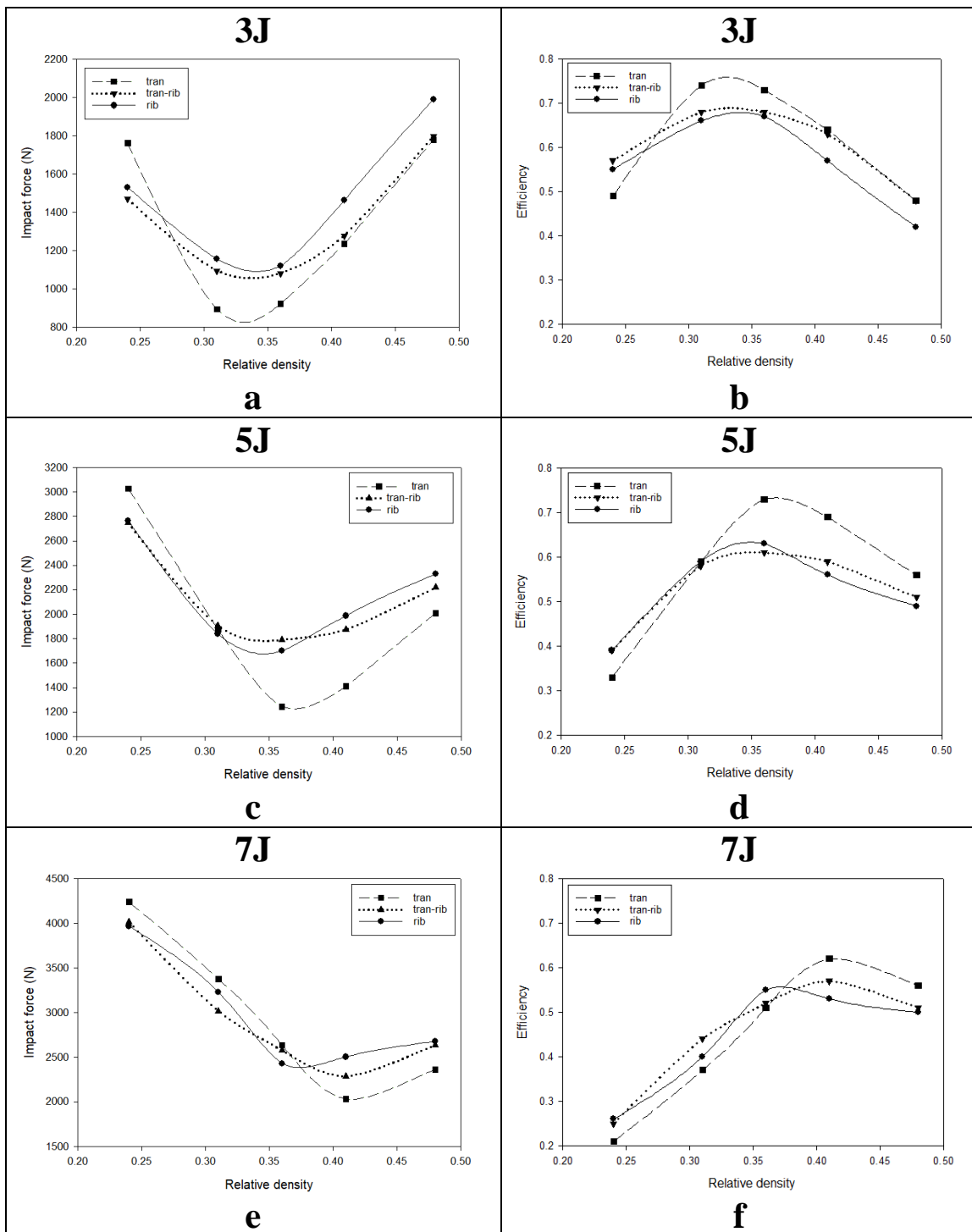


Figure 6, The impact of orientation on honeycomb structures is detailed at specific energy levels: a) at 3J impact force vs ρ_{RD} , b) at 3J displacement vs ρ_{RD} , c) at 5J impact force vs ρ_{RD} , d) at 5J displacement vs ρ_{RD} , e) at 7J impact force vs ρ_{RD} , and f) at 7J displacement vs ρ_{RD} .

Table 1 Mechanical Properties of TPU

Mechanical Properties	Testing method	Typical value
100% modulus	ASTM-D638	9.4±0.3 (MPa)
Tensile strength	ASTM-D638	29.0±2.8 (MPa)
Elongation at break	ASTM-D638	330.1±14.9 (%)
Shore hardness	ASTM-D2240	95A

Table 2 The parameters used for TPU printing parameters.

Parameter	value
Print nozzle diameter (mm)	0.5
Nozzle temperature (°C)	228
Build plate temperature (°C)	50
Cooling Fan	On
Printing Speed (mm/s)	30
Print infill (%)	100
Raft separation distance (mm)	0.2
Retraction distance (mm)	1.0

Table 3 Honeycombs with different angle based on different density

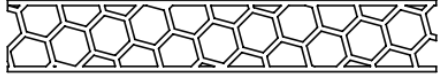
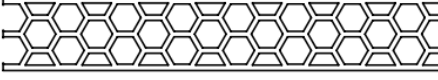
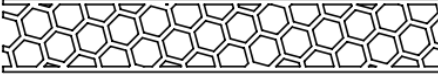
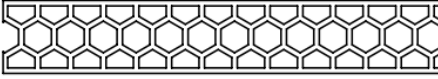
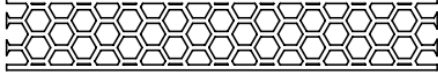
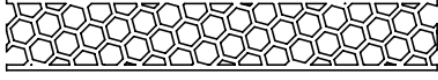
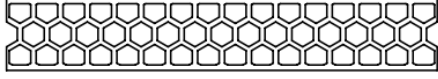
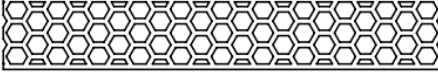
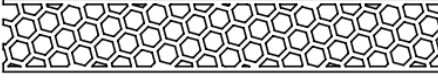
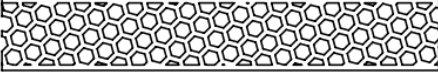
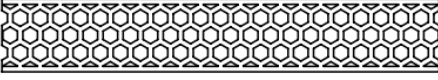
Specimens	Parameter	Angle (Degree)	Thickness and length (mm)	ρ_{RD}
Ribbon-0.24		0	t=0.75 l=3.54	0.24
Tran-Rib-0.24		15		
Transverse-0.24		30		
Ribbon-0.31		0	t=0.75 l=2.81	0.31
Tran-Rib-0.31		15		
Transverse-0.31		30		
Ribbon-0.36		0	t=0.75 l=2.38	0.36
Tran-Rib-0.36		15		
Transverse-0.36		30		
Ribbon-0.41		0	t=0.75 l=2.09	0.41
Tran-Rib-0.41		15		
Transverse-0.41		30		
Ribbon-0.48		0	t=0.75 l=1.80	0.48
Tran-Rib-0.48		15		
Transverse-0.48		30		

Table 4 Physical properties of 3D honeycomb-printed structure

Specimens	Mass (g)	Thickness (mm)	Area (mm²)	Density (g/cm³)
Ribbon-0.24	15.4	9.80	3,555	0.44
Ribbon-0.31	17.2	9.60	3,579	0.50
Ribbon-0.36	20.0	9.85	3,597	0.56
Ribbon-0.41	21.4	9.85	3,570	0.61
Ribbon-0.48	23.9	9.80	3,633	0.67
Tran-Rib-0.24	15.6	10.00	3,570	0.44
Tran-Rib-0.31	17.7	9.90	3,606	0.50
Tran-Rib-0.36	19.7	9.90	3,606	0.55
Tran- Rib-0.41	21.5	9.90	3,591	0.60
Tran- Rib-0.48	23.8	10.00	3,618	0.66
Transverse-0.24	16.1	9.90	3,582	0.45
Transverse-0.31	17.3	9.90	3,564	0.49
Transverse-0.36	18.4	9.90	3,561	0.52
Transverse-0.41	21.7	9.80	3,594	0.62
Transverse-0.48	24.6	9.80	3,573	0.70
Solid TPU-100%	46.7	10.01	3,648	1.29